Department of Veterans Affairs

Journal of Rehabilitation Research and Development Vol. 34 No. 3, July 1997
Pages 279–285

Instantaneous centers of rotation in dorsi/plantar flexion movements of posterior-type plastic ankle-foot orthoses

Tadashi Sumiya, MD; Yoshitaka Suzuki, Eng; Tomio Kasahara, Eng; Hajime Ogata, MD
Rosai Rehabilitation Engineering Center, Nagoya-shi, 455, Japan; Department of Rehabilitation Medicine, University of Occupational and Environmental Health, Kitakyushu-shi, Japan

Abstract—Hingeless plastic ankle-foot orthoses (PAFOs) achieve ankle motion by flexing about the ankle joint. Instantaneous centers of rotation (ICRs) in dorsi- and plantarflexion movements, used as a measure of PAFO axes of movement, were measured to evaluate their fit to ankle motion. Thirty different PAFOs were fabricated and their stiffness modified in three stages. They were dorsi- and plantarflexed 16° at 2°-intervals using an original device. Displacement of two marks on the lateral calf-cuff were traced photographically, and ICRs were determined by plotting intersections of vertical bisectors for each displacement. The ICRs converged on the junction between the calf shell and the shoe insert. They deviated posteriorly from the anatomical ankle axis and caused the calf-cuff to move up-down during dorsi- and plantarflexion movements. However, this poor fit of the PAFO to ankle motion can be sufficiently compensated for by fastening straps more loosely.

Key words: *ankle, instantaneous center of rotation, orthotic device, plastic ankle-foot orthosis.*

INTRODUCTION

Flexible-type hingeless plastic ankle-foot orthoses (PAFOs) allow controlled dorsi- and plantarflexion movements of the ankle by flexing and extending the orthotic body. These bending movements usually result not only in considerable deformation around the ankle but also in piston movement of the calf-cuff. The vertical movement of the calf-cuff is thought to be attributable to failure of the most flexible portion of PAFOs to coincide with the anatomical ankle axis. However, the precise axis of dorsi- and plantarflexion movements is still unclear, since the hingeless PAFO displays flexibility throughout its entire body.

PAFOs that always flex congruently with the actual ankle movement of the body during walking (dynamic orthosis-body fit) are more comfortable. Application of independent ankle joint structures to PAFOs is most effective in achieving dynamic fit, but has the drawback of bulkiness or cosmetic problems. Hingeless PAFOs, on the other hand, provide poorer dynamic fit but are more compact and cosmetically acceptable than hinged PAFOs (1). The degree of dynamic fit of hingeless PAFOs may vary according to their basic design (depending on whether they are the posterior-type, lateral-type, or anterior-type), because patterns of deformation vary with structure. These differences in degree of dynamic fit between basic designs can be useful in classifying the characteristics of hingeless PAFOs to enable proper prescription.

The objective of this research was to determine the axis of dorsi- and plantarflexion movements with posterior-type PAFOs, the most familiar basic design, and to assess their dynamic orthosis-body fit, based on the con-

This material is based upon work supported by a grant from the Japanese Labor Welfare Corporation.
Address all correspondence and requests for reprints to: Tadashi Sumiya, MD, Rosai Rehabilitation Engineering Center, 1-10-5 Komei, Minato-ku, Nagoya-shi, 455, Japan.

Journal of Rehabilitation Research and Development Vol. 34 No. 3 1997

viction that orthotic and body axes should be congruent. Instantaneous centers of rotation (ICRs) were regarded as representing the axis of hingeless PAFOs in this study. Since degree of flexibility varies greatly even within the posterior-type category, the orthoses were trimmed in three stages, and the influence of trimming on the location of the ICRs was evaluated. Furthermore, the extent of calf-cuff piston movement was measured to observe the degree of poor orthosis-body dynamic fit.

METHODS

Two experienced orthotists fabricated 30 PAFOs, 24 for clients and 6 for able-bodied adults, using 3-mm thick standard-grade polypropylene and the vacuum-forming technique. The proximal trim line was set 2.5 cm below the fibular head, and the metatarsal trim line was extended to the tip of the toes.

Before making the experimental settings, it was decided to locate the fixed ankle axis horizontally at lateral malleolus height, perpendicular to the midline of the foot at the intersection with the bimalleolar line (the line connecting the midpoints of the lateral and medial malleoli; see **a** in **Figure 1**). This axis governed trim line configurations and served as a fulcrum for bending the orthoses with the lever.

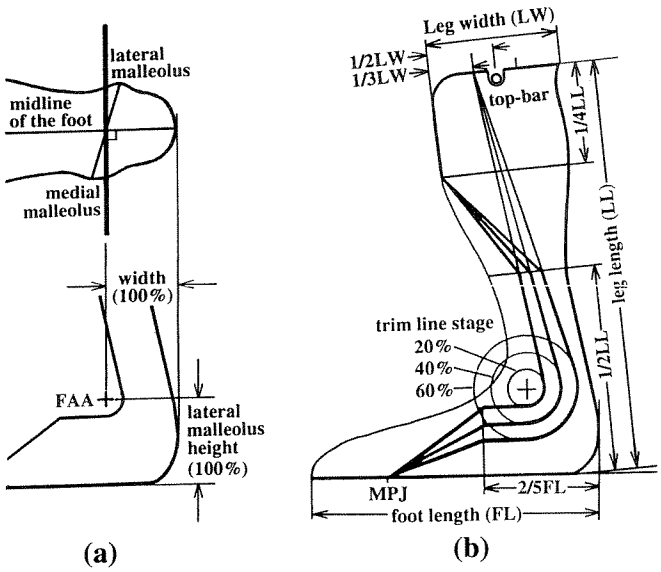

Figure 1.
a. The fixed ankle axis, height: the distance between the midpoint of the lateral malleolus and the out-sole of the shoe insert, width: the distance between the axis and the posterior heel edge. The height and the width are equalized to 100% when ICR coordinates are standardized.
b. The three-stage trim line configurations.

Isman and Inman (2) reported that the mean angle between the axis of the talocrural joint and the midline of the foot was 84°, SD 7°, the mean angle between the axis of the talocrural joint and the axis of the tibia was 80°, SD 4°, hence the fixed ankle axis in this study was rotated about 6° medially and pronated about 10° with respect to the anatomical ankle axis. Although it has been accepted worldwide that the orthotic ankle axis should coincide with the anatomical ankle axis (3–9), we question this thinking. The ankle and the subtalar joints are always interdependent and in general act as a unit during walking (10). Therefore, orthotic ankle joints that are perfectly congruent with the anatomical ankle axis can theoretically produce unnatural ankle motion by allowing the talocrural joint alone to move, while simultaneously impeding subtalar joint motion (11). Clinical experience supports this theory and has suggested the suitability of the ankle axis location shown in **a** in **Figure 1.** However, this orthotic ankle axis cannot be considered absolute, because the subjects are biased toward stroke and spinal cord injury victims alone and because this orthotic ankle axis is of necessity influenced by such factors as spasticity, range of motion, deformity, and activity level.

The ankle trim lines consisted of arcs of circles and their tangents. The centers of the circles were positioned on the fixed ankle axis. The tangents and other straight lines were extended to complete the entire trim line according to the dimensions of the orthosis (**b** in **Figure 1**). Three different radii, equal to 20, 40, and 60 percent of lateral malleolus height, provided the three-stage trim lines, and thus orthotic hardness was altered from semirigid (20 percent) to flexible (60 percent). Measurements of ICRs were performed repeatedly after each trim line modification for all PAFOs fabricated in this study.

Plaster foot models molded for each PAFO were set into the shoe insert to maintain the orthotic sole flat and horizontal, and they were provided with a single-axis joint at the location of the fixed ankle axis. Orthoses and foot models were anchored together on a table with screws (**a** in **Figure 2**). The calf-cuff portion of the orthoses was kept empty to avoid the influence of weight loading by the calf-model and to allow as free a deformation as possible to reproduce natural deformation, which is usually maximized by sufficient space under the calf-cuff and the softness of the body, in general use. A lever was used to bend the orthoses manually. The fixed ankle axis served as the fulcrum, and a metal top bar, set in the

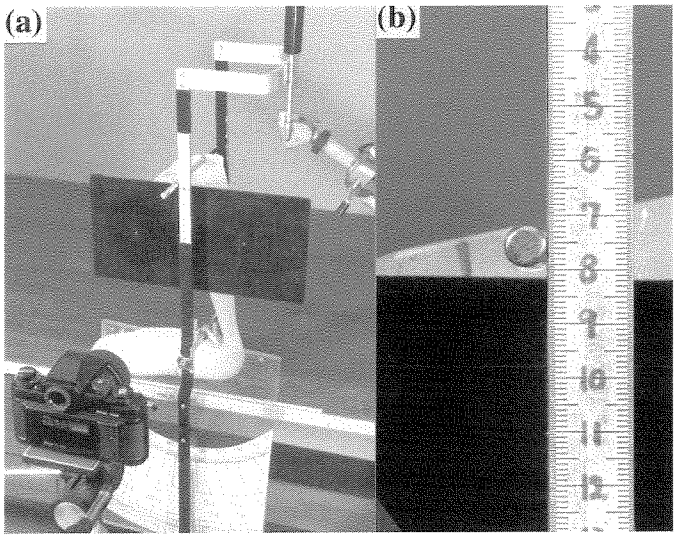

Figure 2.
a. The device used to dorsi- and plantarflex the PAFOs. This photograph shows the setting for dorsiflexion movement. Force is applied to the lever through a tripod fixed with a vise. The top bar is positioned behind the lever in the setting for plantarflexion movement. **b.** The scales on the lever to measure the sliding distance of the top bar.

middle portion of the proximal calf-cuff parallel to the axis, served as the point of action (**b** in **Figure 1** and **a** in **Figure 2**). Furthermore, the lever was equipped with scales to measure the extent of vertical sliding movement of the top bar during dorsi- and plantarflexion movements (**b** in **Figure 2**). Using this device, the extent of pistoning in 60 percent-trimmed PAFOs was measured concurrently with ICR measurements.

The orthoses were both dorsi- and plantarflexed 16° at intervals of 2°, with 2 spot marks placed on the lateral side of the calf-cuff so that they moved in the sagittal plane of the foot (the vertical plane that includes the midline of the foot). Lateral views of the orthoses were photographed with a still camera, with the optical axis set parallel to the fixed ankle axis. Each spot displaced when the orthoses were flexed from a certain ankle angle a° to the other angle b°, and perpendicular bisectors were drawn for each pair of displacements (**Figure 3**). The intersection of the bisectors, ((a+b)/2)°, determined the position of the ICR at the particular ankle angle (12). The ICR at 5° was obtained from the intersection of bisectors between 4° and 6° (2° interval), and the ICR at 10° was obtained from the intersection of bisectors between 8° and 12° (4° interval) in both dorsi- and plantarflexion movements. In the accuracy test performed prior to this study, the error in actual size was ±3.2 mm in the 2° interval method and ±2.9 mm in the 4° interval method.

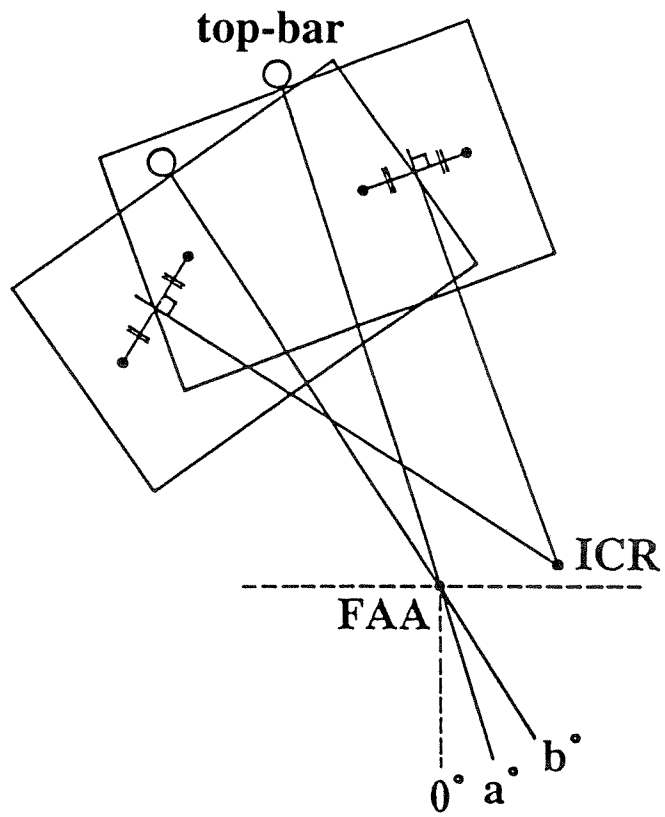

Figure 3.
The construction for determining the ICR. When two marks shift from a certain ankle angle a° to b°, the intersection of vertical bisectors determines the ICR at the particular ankle angle ((a+b)/2)° FAA: fixed ankle axis.

The difference in errors between the two methods could be ignored, and ICRs at 5° and 10° were treated equally.

The locations of the ICRs were initially expressed as actual values of the X and Y coordinates with their origin on the fixed ankle axis, and they were standardized by setting both the height and the width of the axis at 100 percent (**b** in **Figure 1**). Namely, each ICR coordinate was expressed as a percentage of the height and the width of each PAFO so that the ICRs of 30 PAFOs of various sizes could be compared to each other on the same coordinate. Differences in the population mean of the X and Y coordinates between dorsi- and plantarflexion movements (ankle angle and trim line stage were matched in the ICR groups), 5° and 10° of ankle angle (ankle position and trim line stage were matched in the ICR groups), and different trim line stages (ankle angle and position were matched in the ICR groups) as well, were statistically tested by using the two-sample *t*-test with Welch's correction ($p<0.05$) to assess the degree of transverse and

Journal of Rehabilitation Research and Development Vol. 34 No. 3 1997

vertical deviation of ICRs from the fixed ankle axis. Differences in the population variance of the X and Y coordinates between the same pairs of ICR groups as above were tested by using the F-statistic ($p<0.05$) to assess the relative degree of transverse and vertical dispersion in each ICR group.

RESULTS

Although the semi-rigid PAFOs in this study were forced into a considerable degree of plantar flexion, no abnormal deformation, such as folding or twisting, was observed over the calf shell. The relative force required to gain an equal ankle angle of dorsi/plantar flexion with these PAFOs was approximately one half, as has been previously reported (13).

The standardized X and Y coordinates of the ICRs under 12 different conditions are shown in **Table 1,** and they are illustrated in **Figure 4.** Most of the ICRs were dispersed over the junction between the calf shell and the shoe insert (junction region) under all conditions. The mean location and dispersion of the ICRs varied depending on ankle position, ankle angle, and trim line stage.

Regarding the transverse ICR distribution, dorsiflexion movement created significantly further backward ICR deviation than plantarflexion movement in the 20 percent-trimmed PAFOs alone. The mean ICR location shifted significantly backward when trim line stage increased in plantarflexion movement. Dorsiflexion movement caused significantly wider ICR scatter than plantarflexion movement. The degree of ICR dispersion did not show constant correlation with the trim line stage. Ankle angle did not influence the transverse location and dispersion of the ICRs significantly.

Regarding the vertical ICR distribution, plantarflexion movement generated the mean ICR location at approximately the same height as the fixed ankle axis, but dorsiflexion movement tended to produce significantly lower mean ICR location than plantarflexion movement in all cases. The vertical ICR distribution also showed significantly wider ICR scatter in dorsiflexion movement than in plantarflexion movement. The vertical ICR location and dispersion did not show constant correlation with trim line stage. Ankle angle did not influence the vertical location and dispersion of the ICRs significantly.

ICR distribution can be roughly characterized as follows. The major findings were mean ICR convergence over the junction region (**a** in **Figure 4**), and wider dispersion in dorsiflexion movement than in plantar flexion movement (**b** and **c** in **Figure 4**). The minor findings were the lower location of mean ICRs in dorsiflexion movement than in plantarflexion movement (**b** and **c** in **Figure 4**), and trimming-dependent backward shifts of ICRs in plantar flexion movement (**d** in **Figure 4**).

The extent of vertical sliding movement of the top bar with 60 percent-trimmed PAFOs is shown in **Figure 5.** The mean distance of pistoning in dorsi/plantarflexion movements was 1.9/4.1 mm at 6°, 6.8/6.9 mm at 10°, and 10.2/11.3 mm at 16°. Namely, the maximum calf-cuff sliding distance was as much as 21 mm within 32° of ankle angle range, equivalent to approximately 6 percent of the orthotic leg length.

Table 1.
Standardized ICR coordinates.

Trim line		DF 10°		DF 5°		PF 5°		PF 10°	
Stage		X	Y	X	Y	X	Y	X	Y
20%	Mean	83.5	−30.7	77.8	−32.6	61.9†	−5.95	64.8‡	5.42
	SD	24.8	27.8	22.2	30.3	13.4	20.5	16.8	22.8
40%	Mean	79.9	−16.0	74.9	−16.8	71.2†	7.75	75.6‡	13.7
	SD	30.6	43.4	26.6	35.4	14.7	15.7	15.1	17.6
60%	Mean	81.2	−20.0	78.4	−15.0	82.6†	5.17	85.5‡	5.76
	SD	21.8	30.5	17.1	25.7	18.5	14.6	17.8	19.4

DF: dorsiflexion; PF: plantar flexion. All values are expressed as percentages. The origin of X-Y coordinate locates on the fixed ankle axis. † and ‡ indicate significant differences between trim line stages at $p<0.05$ level.

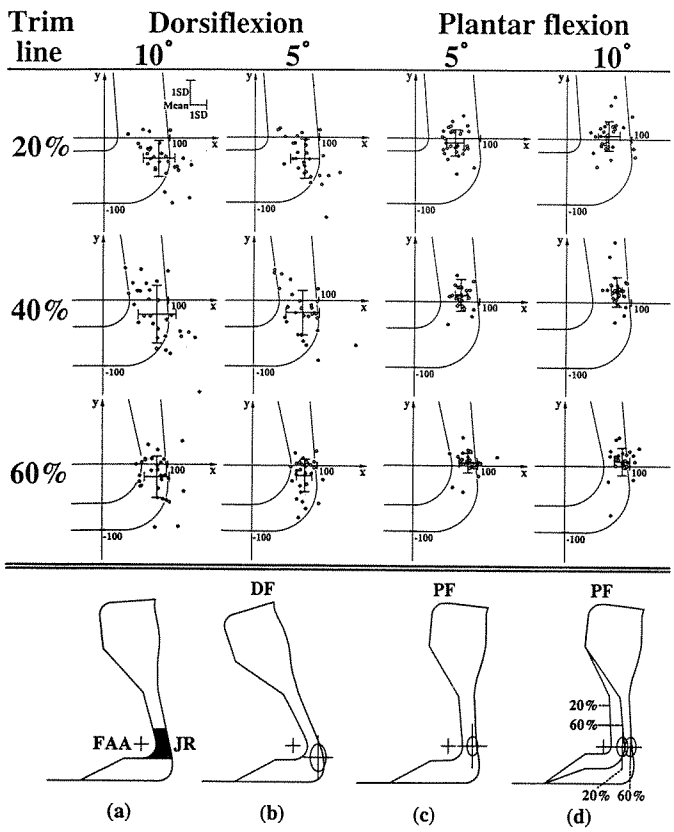

Figure 4.
Top: the standardized ICRs at 5° and 10° in dorsi- and plantarflexion movements plotted on the X and Y coordinates as percentages. Bottom: illustration of characteristic findings in the ICR distribution, **a.** mean ICR convergence on the junction region; **b, c.** wider dispersion and lower location of ICRs in DF than PF; **d.** trimming-dependent backward shifts of ICRs in PF. FAA: fixed ankle axis, JR: junction region, DF: dorsiflexion movement, PF: plantarflexion movement.

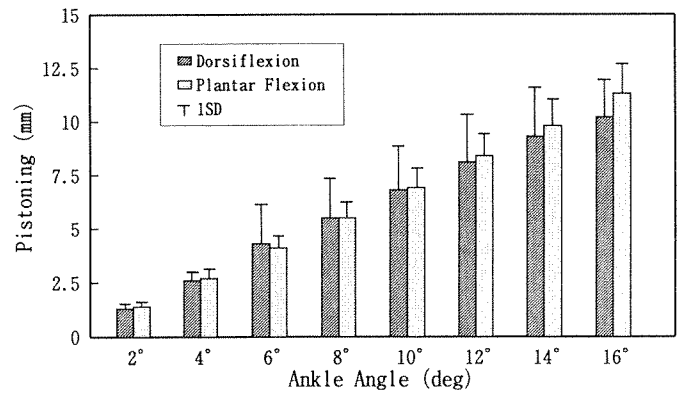

Figure 5.
The extent of calf-cuff pistoning with 60%-trimmed PAFOs.

DISCUSSION

The results indicate that this type of PAFOs has variable axes for dorsi- and plantarflexion movements that range throughout the junction region, because the junction region has the narrowest width and thus is the most flexible.

While plantarflexion movement deflects the junction region posteriorly as a result of tensile force and results in ICR convergence over the same area, dorsiflexion movement causes bilateral bulging of the broader area from the junction region to the proximal portion of the shoe insert as a result of compressive force and results in lower ICR distribution. The structural complexity of this bulge in dorsiflexion movement makes individual differences in ICR location larger than in plantarflexion movement.

Additional trimming made the junction region thinner, shifting the ICRs to the posterior edge of the calf shell in plantarflexion movement. This backward shift in ICR location may slightly worsen the poor dynamic fit. However, the increased flexibility over the entire calf shell, not only in dorsi/plantarflexion movements but in inversion/eversion and internal/external rotation movements as well, can serve to buffer the poorer dynamic fit of PAFOs in natural use.

The fact that the fixed ankle axis location and the empty calf-cuff influenced the results to a greater or lesser extent cannot be ignored. However, the absence of abnormal deformation over the calf shell, such as folding or twisting, indicates that the fixed ankle axis location and the empty calf-cuff in this study were the preferable experimental conditions for the best reproduction of the natural orthotic deformation during walking. Dorsi- and plantarflexing the PAFOs using the fixed ankle axis worked to create less asymmetrical strain over the calf shell than using the anatomical ankle axis that rotated externally with respect to the midline of the foot. On the other hand, although the empty calf-cuff can make the PAFO more flexible than in natural use, unloading made the orthotic deformation as natural as possible.

The backward deviation of ICRs from the fixed ankle axis is chiefly responsible for calf-cuff piston movement during walking: upward sliding in plantarflexion movement and downward sliding in dorsiflexion movement. The results indicated that considerable calf-cuff pistoning could occur when flexible PAFO-braced persons walk with a wide range of ankle motion. This

manifestation of dynamic poor fit is often seen clinically in subjects wearing this type of PAFO.

Two techniques are known to be effective in minimizing friction and chafing under the calf-cuff: the sliding attachment used for the VAPC shoe clasp orthosis (14) and the plastic inner cuff adopted for posterior leaf-spring orthoses (15). However, these techniques have not been adopted generally for posterior-type PAFOs. Comfortably fastened calf-, ankle-, and foot-straps can provide appropriate play between the orthosis and the body, sufficiently buffering the poor dynamic fit of the PAFO and preventing irritating friction under the calf-cuff.

Persons braced with Japanese-style PAFOs (**a** in **Figure 6**) often complain of ankle pain during walking. This results from their completely preventing calf-cuff piston movement with ankle- and foot-straps and can be successfully relieved by loosening them. On the other hand, lacing the shoe so that it allows appropriate play is effective in compensating for the poor dynamic fit in Western-style PAFOs (**b** in **Figure 6**). The problem of strap-induced pain is less likely to occur when people wear shoes inside (the Western style) than when people remove their shoes when they enter houses (the Japanese style), because the shoe joins the foot and the PAFO by ensheathing them more effectively than ankle- and foot-straps, and thus unshod persons tend to tighten the straps more firmly to keep the foot/PAFO complex stable.

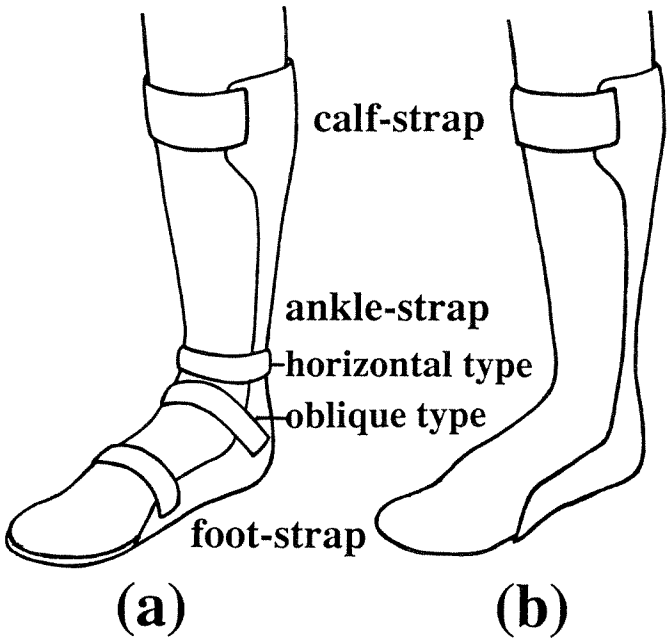

Figure 6.
Strap attachment: **a.** Japanese style; **b.** Western style.

However, play cannot compensate for poor dynamic orthosis-body fit when firm fixation of the orthosis to the body is needed to strictly control ankle/foot motion. The use of PAFOs equipped with independent ankle joint structures is a substitute in such cases, but they alone are unsatisfactory, because even hinged PAFOs deflect their body when the ankle motion exceeds the flexible range of the orthotic joint structure. In such circumstances, shoes modified to absorb the shock of heel-striking should be effective in reducing the range of plantarflexion movement during the stance phase and consequently minimizing poor dynamic orthosis-body fit. Articulation is also required when adjusting the resistance to dorsi- or plantarflexion movements to improve discomfort resulting from hyperrigidity during the use of PAFOs.

Differences between the dynamic orthosis-body fit of various hingeless PAFO designs should be clarified and functionally evaluated in future studies.

CONCLUSION

Posterior-type hingeless PAFOs focus instantaneous centers of dorsi- and plantarflexion movements on the junction between the calf shell and the shoe insert, and the centers of these movements are deviated backward from the standard orthotic ankle axis, thereby causing considerable extent of calf-cuff piston movement during walking. However, this poor dynamic orthosis-body fit can be satisfactorily compensated for by loosely fastening the calf-, ankle- and foot-straps or lacing the shoe to allow appropriate play, and the omnidirectional flexibility of plastic provides an additional buffer. However, PAFOs should be articulated when strict control of ankle/foot motion or adjustment of orthotic stiffness is needed.

ACKNOWLEDGMENTS

The authors are grateful for the assistance of Minoru Nakamura and Hideshi Shibayama, Watanabe Orthotics & Prosthetics Co. Ltd., in fabricating the orthoses.

REFERENCES

1. Murray WT, Greenfield JE. The cosmetic below-knee brace. Orthot Prosthet 1970:24:27–30.
2. Isman RE, Inman VT. Anthropometric studies of the human

foot and ankle. Bull Prosthet Res 1969:BPR10-11:97–129.
3. Stamp WG. Bracing in cerebral palsy. Orthot Prosthet 1963:17:354–73.
4. Lehneis HR. Brace alignment considerations. Orthot Prosthet 1964:Dec:110–4.
5. Lusskin R. The influence of errors in bracing upon deformity of the lower extremity. Arch Phys Med Rehabil 1966:47:520–5.
6. Inman VT. UC-BL dual-axis ankle-control system and UC-BL shoe insert: biomechanical considerations. Bull Prosthet Res 1969:BPR10-11:130–45.
7. Lamoreux LW. UC-BL dual-axis ankle-control system: engineering design. Bull Prosthet Res 1969:BPR10-11:146–83.
8. Glancy J. Brace-to-body dynamics. Orthot Prosthet 1970: 24:21–9.
9. Bahler A. Principles of design for lower limb orthotics. Orthot Prosthet 1982-3:36:33–9.
10. Wright DG, Desai SM, Henderson WH. Action of subtalar and ankle-joint complex during the stance phase of walking. J Bone Joint Surg 1964:46-A:361–83.
11. Kubota T. Abnormal gait patterns in stroke patients with hemiplegia and their correction with lower-extremity orthotics: biomechanical considerations. In: The Japanese Society of Prosthetics and Orthotics. Lower extremity orthotics for stroke patients with hemiplegia. Tokyo: Ishiyakushuppan, 1981: 33–48.
12. Frankel VH, Burstein AH, Brooks DB. Biomechanics of internal derangement of the knee. J Bone Joint Surg 1971:53-A:945–62.
13. Sumiya T, Suzuki Y, Kasahara T. Stiffness control in posterior-type plastic ankle-foot orthoses: effect of ankle trimline. Part 2: orthosis characteristics and orthosis/patient matching. Prosthet Orthot Int 1996:20:132–7.
14. Rubin G, Dixon M. The modern ankle-foot orthoses (AFOs). Bull Prosthet Res 1973:BPR10-19:20–41.
15. Rubin G, Danisi M. A "slip" cuff for ankle-foot orthoses—a piston-action absorbing polypropylene orthotic cuff. Orthot Prosthet 1974:28:43–4.

Submitted for publication February 20, 1995. Accepted in revised form December 10, 1996.